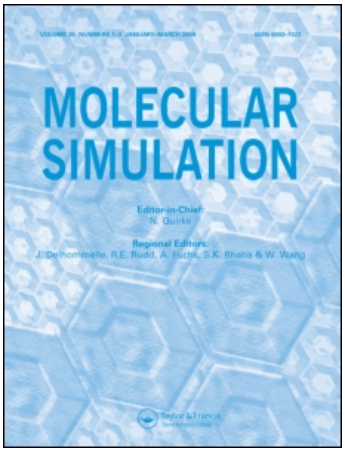

Molecular Simulation
Publication details, including instructions for authors and subscription information:
http://www.informaworld.com/smpp/title~content=t713644482

DFT study of conductive properties of three polymers formed by bicyclic furans

Xiaohua Xie[a]; Wei Shen[a]; Yangwu Fu[ab]; Ming Li[a]
[a] School of Chemistry and Chemical Engineering, Southwest University, Chongqing, P.R. China [b] Department of Chemical and Environmental Engineering, Chongqing Three Gorges University, Chongqing, P.R. China

Online publication date: 15 October 2010

To cite this Article Xie, Xiaohua , Shen, Wei , Fu, Yangwu and Li, Ming(2010) 'DFT study of conductive properties of three polymers formed by bicyclic furans', Molecular Simulation, 36: 11, 836 — 846
To link to this Article: DOI: 10.1080/08927022.2010.482136
URL: http://dx.doi.org/10.1080/08927022.2010.482136

Molecular Simulation
Vol. 36, No. 11, September 2010, 836–846

Taylor & Francis
Taylor & Francis Group

DFT study of conductive properties of three polymers formed by bicyclic furans

Xiaohua Xie[a], Wei Shen[a], Yangwu Fu[ab] and Ming Li[a]*

[a]*School of Chemistry and Chemical Engineering, Southwest University, Chongqing 400715, P.R. China;* [b]*Department of Chemical and Environmental Engineering, Chongqing Three Gorges University, Chongqing 404000, P.R. China*

(*Received 16 August 2009; final version received 29 March 2010*)

Density functional theory methods were employed to study the electronic, structural and conductive properties of classical bicyclic furans. In this paper, studies of monomers, oligomers and polymers of furo[3,4-*b*]furan, furo[2,3-*b*]furan and furo[3,2-*b*]furan are presented. To gain detailed information on conjugational degree, we selected the nucleus-independent chemical shift as a method for examining the changes in conjugational degree. Furthermore, three parameters of density of state, effective mass (m^*) and kinetic model of mobility (μ) were also investigated. The variable trends of all parameters from monomers to tetramers indicate that poly(4,4′-bifuro[3,4-*b*]furan), poly(*trans*-2,2′-bifuro[3,2-*b*]furan) and poly(*cis*-2,2′-bifuro[3,2-*b*]furan) are good candidates for conductive materials, which are consistent with band structure analyses showing that the three polymers had narrower band gaps (1.21, 1.93 and 1.89 eV, respectively) than other polymers.

Keywords: bicyclic furans; electronic structure; nucleus-independent chemical shift; effective mass

1. Introduction

Many researchers have devoted themselves to studying π-conjugated polymers since the finding that doped π-conjugated polymers have metallic conductive properties [1,2]. More and more scientists have synthesised such kinds of polymers, which have become the focus of interest [3–6]. Because the size of the energy gap embodies the conductive property, finding such polymers with small band gaps is an important goal. Currently, there are many ways in which we can reduce polymer band gaps, such as newly doped molecules, new conformational structures and so on. However, the two key steps may be (1) exploring parent molecules with low-energy gaps and (2) exploring the relationship between the energy gap and the electronic properties of monomers and oligomers. The latter way is more helpful for designing conductive molecules because the electronic properties of monomers and oligomers are closely related to polymer band gaps [7].

In this paper, three classical bicyclic furans are selected as parent molecules: furo[3,4-*b*]furan (**Fa**), furo[2,3-*b*]furan (**Fb**) and furo[3,2-*b*]furan (**Fc**). These bicyclic furans may form six polymers: poly(4,4′-bifuro[3,4-*b*]furan) (**1PFa**), poly(3,6′-bifuro[3,4-*b*]furan) (**2PFa**), poly(2,2′-bifuro[2,3-*b*]furan) (**PFb**), poly(*trans*-2,2′-bifuro[3,2-*b*]furan) (**1PFc**), poly(*cis*-2,2′-bifuro[3,2-*b*]furan) (**2PFc**) and poly(3,3′-bifuro[3,2-*b*]furan) (**3PFc**), respectively. Nowadays, some furofurans and their derivatives are synthesised successfully [8,9]. **Fa** was synthesised with cyclopropa-1,2-diene in 1986 [10], and Vader and his co-workers [11] found that dialkylated aldehyde furnished **Fb** under the condition of acid-catalysed cyclisation after three years; meanwhile, some derivatives of **Fc** have also been reported [12].

In the present work, we intend to understand conductive properties of the above-mentioned polymers by examining the types of transtactic block polymerisation, the intrinsic and electronic structures of oligomers, and the change in trends of electronic and structural properties from monomers to tetramers. These systems that we select have no steric repulsion between the adjacent heterocyclic units leading to a planar geometry, and each molecule has high electron affinity which is attributed to oxygen atoms, and that may be helpful for their polymers embodying better qualifications for forming conductors.

As for organic compounds, strong conjugation degree and aromaticity are important properties for conductive ability. Hence, conjugation degree and aromaticity can embody conductive ability to a certain degree. We select the nucleus-independent chemical shift (NICS) [13] as a method for examining the changes in conjugational degree by calculating NICS values of the ring critical points (RCPs). Furthermore, the band gaps, density of state (DOS) and effective mass (m^*) along with the kinetic model of mobility (μ) are also investigated.

2. Computational details

In this paper, we explain the qualitative features by employing the density functional theory (DFT) [14] to obtain insight into molecular design; the Becke's

*Corresponding author. Email: liming@swu.edu.cn

ISSN 0892-7022 print/ISSN 1029-0435 online

DOI: 10.1080/08927022.2010.482136
http://www.informaworld.com

three-parameter non-local exchange function with the Lee–Yang–Parr non-local correlation function (B3LYP) [15,16] is used to optimise all the structures of monomers and oligomers. All the structures have no imaginary frequencies at the present level, which implies that all the optimised structures are the steady points on the reaction potential energy surface. The block polymers are calculated using the periodic boundary condition (PBC) method [17]. 6-31G*, a moderate basis set, is used throughout all optimisations, and all calculations are carried out by Gaussian 03 package [18]. On the basis of the optimised structures, monomers, oligomers and polymers are studied by employing electronic density topological analyses and NICS calculation at the B3LYP/6-31G* level. Electronic density topological analyses are obtained using atom-in-molecule (AIM) analyses [19]. The NICS method was used widely to assess the aromaticity and anti-aromaticity of many compounds. In this paper, NICS is defined as the negative of the magnetic shielding at an RCP and at 1.0 Å above the RCP, which is obtained from the AIM analyses.

In order to discuss the electronic and structural characters well, we extract one isolated structure from a block polymer structure for each polymer. The single-point calculation including full population analysis is explored at the B3LYP/6-31G* level on the basis of the optimised structure, DOS is performed and the DOS graph is obtained from GaussSum 1.0 [20,21].

3. Results and discussion

3.1 Monomer and oligomer

The structures and geometrical parameters of optimised parent molecules of **Fa**, **Fb** and **Fc** are shown in Figure 1. In this paper, the central bond is denoted as the C—C bond which connects two neighbouring central rings, and the sketch of studied compounds is shown in Scheme 1 (e.g. in the **1Fa** dimer, the central bond is the bond C1 that connects b1 and b2 rings; in the **1Fa** tetramer, the central bond is the bond C2 that connects b2 and b3 rings). The bond critical point (BCP) properties, Wiberg bond indices (WBIs) [22] and central bond lengths of the central bonds of the studied compounds are listed in Table 1. From Table 1, we can see that the central bond length decreases with increasing polymeric number. At the same time, the complete topological analyses for all compounds are given in Table 1. BCPs, which represent saddle points between two atoms, are denoted as (3, −1), and they are examined for all the bonds. In order to obtain more detailed bond properties, the charge densities $P_{(r)}$, Laplacian ($\nabla^2_\rho(r)$) and eigenvalues of the Hessian matrix (λ_i) at the BCPs are also listed in Table 1. The charge densities $P_{(r)}$ and the Laplacian ($\nabla^2_\rho(r)$) inspect the changes in electronic accumulation [23]. As shown in Table 1, the central bond densities (more positive) and the Laplacian ($\nabla^2_\rho(r)$) (more negative) of the compounds increase with the increase in polymeric number, which illustrates that the local populations of charges in those bonds increase, and all the above data show that the conjugational degree of compounds increases with the increase in polymeric number. Moreover, the parameters ϵ_{BCP} and WBIs are used to measure the π-bond character. Based on the AIM theory, the larger the ϵ_{BCP} value, the stronger the conjugation. The WBIs in Table 1 are between 1.0 and 2.0, and they display π-bond characters. Also, from Table 1, it can be seen that ϵ_{BCP} and WBIs increase with the increase in polymeric number, which shows strong π-bond features of the central bonds. However, the ϵ_{BCP} of **1PFa** is not the largest in its system, as well as for **PFb**, **1PFc** and **2PFc**, the reason being that the ϵ_{BCP} values of **PFa**, **PFb** and **PFc** are from one selected isolated structure, respectively, as we cannot calculate the ϵ_{BCP} of

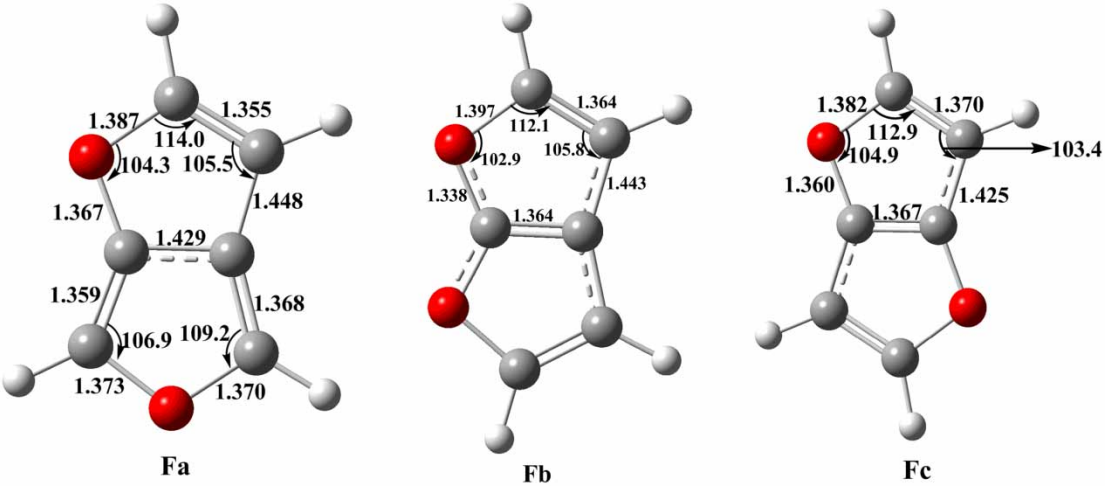

Figure 1. Optimised structures of monomeric molecules, along with bond lengths (in Å) and angles (in °).

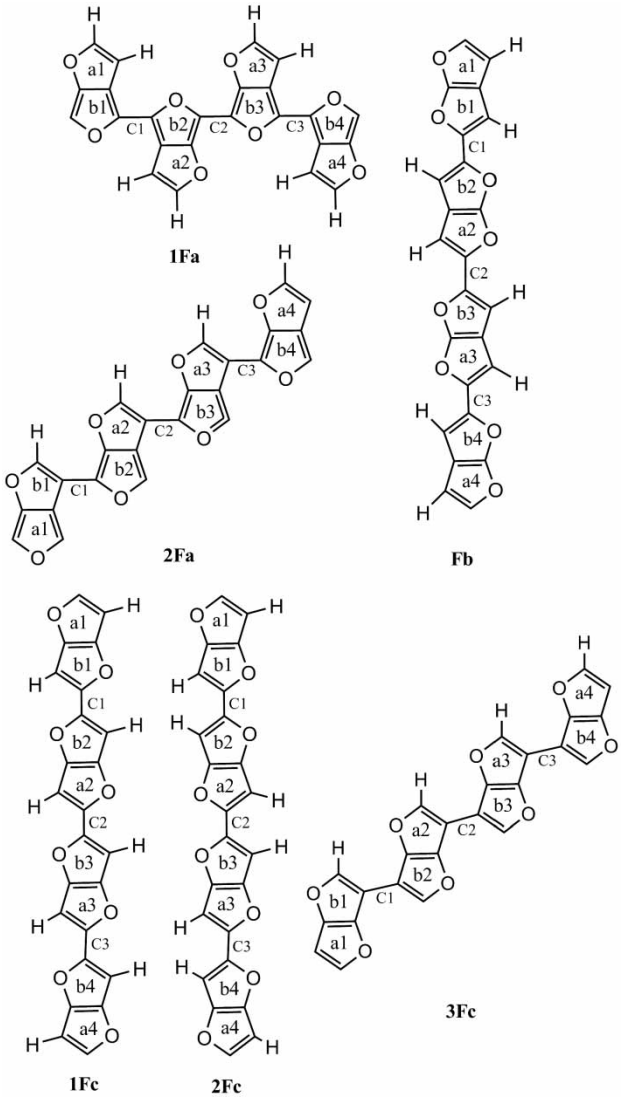

Scheme 1. Sketch of the studied compounds.

a whole polymer at present; after all, the selected segment is different from the whole molecule. Furthermore, the charge of the C atom in the central bond is almost more positive (**1Fa**, −0.015 → 0.203 → 0.265 → 0.286; **2Fa**, −0.015 → 0.282 → 0.285 → 0.286; **Fb**, 0.061 → 0.267 → 0.267 → 0.263; **1Fc**, 0.06 → 0.259 → 0.259 → 0.258; **2Fc**, 0.06 → 0.256 → 0.255 → 0.255; **3Fc**, 0.06 → 0.091 → 0.092 → 0.093), which suggests that the charges are transferred from the C atom to the central bonds with the increase in polymeric number.

The NICS was used diffusely to express the aromaticity of molecules, since the NICS can distinctly and simply monitor the condition of ring currents, which was mainly used to represent the π-electron delocalisation by examining the NICS values at differently positioned rings in the molecular system. Moreover, the changes in NICS at differently positioned rings in the polymer can indicate the conjugational degree. It is a rule that systems with large negative NICS values are aromatic and those with strong positive NICS values are anti-aromatic. Therefore, non-aromatic cyclic systems should have the NICS values close to zero [24]. In this paper, the NICS was selected as a model system to understand the relationship between conjugational degree and ring current density. Generally speaking, NICS is computed at the ring centre, namely at the position of the RCP (NICS (0 Å)), and it can also be calculated at a certain distance above or below the centre of the ring. It was reported that the NICS value computed at 1.0 Å above the RCP (NICS (1.0 Å)) is recommended as being a better measure of π-electron delocalisation when compared with that of NICS (0 Å) [24,25]. Hence, in the present work, both NICS (0 Å) and NICS (1.0 Å) values for monomers and oligomers are calculated and listed in Table 2. The positions of all the rings are shown in Scheme 1.

Meanwhile, the NICS (0 Å) and NICS (1.0 Å) values of furan are also calculated at the same level, which are 13.2 and 10.2 ppm, respectively. The values in Table 2 illustrate that all of the studied compounds have strong local aromaticity, and most of the NICS values in the central section in monomers and oligomers are smaller than those in the sole furan. It indicates that polymerisation makes the electronic ring current to decrease.

The values in Table 2 show that the change in NICS values from the same parent molecule in the terminal ring is small. For example, for **Fb**, the values of a1 from monomer to tetramer are approximate, which are 8.8, 8.5, 8.5 and 8.5 ppm, and the results suggest that the ring current in the terminal ring just influences the central section slightly. For the side rings (position **a**), the NICS values change slightly as well, such as the a1, a2 and a3 values in the **1Fa** trimer are 6.3, 6.4 and 6.4 ppm, respectively, indicating a change of only 2%. Furthermore, the NICS values in the terminal and side rings change slightly with the increase in polymeric number, which indicates that the central electronic ring currents have less effect on the terminal and side rings. The reason is that ring a is far from the polymeric axis, and the polymeric number just slightly influences the ring current [7].

Along the polymeric axis, the NICS values decrease obviously, for example the values of **1Fa**-b1 from monomer to tetramer are 10.9, 9.3, 9.1 and 9.1 ppm. In the central sections, the change in NICS values is also evident. In the tetramer of **1Fa**, the NICS values of b1 and b2 are 9.1 and 7.9 ppm, respectively, and the values change more evidently. The reason for the above results is that b2 is not only close to the polymeric axis, but also close to the centre of the molecule. However, in the case of **Fb** and **Fc**, the ring currents in the central rings are smaller than those at the terminal ones; for example, in the trimer of **Fb**, the NICS values are 8.5, 7.6, 7.4 and 7.4 ppm; in the tetramer of **1Fc**, they are 8.8, 8.0, 7.7 and 7.6 ppm. For **2Fa** and

Table 1. BCP properties and Wiberg bond index of the central bond[a] of the studied compounds.

	Polymeric number	$P_{(r)}$	$(-\lambda_1)/(-\lambda_2)/\lambda_3$	$\nabla^2_\rho(r)$	ϵ_{BCP}	Central bond length (Å)	WBIs[b]
1Fa	Dimer	0.299	0.65/0.52/0.35	−0.822	0.262	1.426	1.144
	Trimer	0.301	0.65/0.52/0.35	−0.832	0.274	1.421	1.161
	Tetramer	0.301	0.66/0.51/0.35	−0.825	0.284	1.418	1.161
	Polymer[c]	0.309	0.69/0.57/0.35	−0.913	0.208	1.409	1.460
2Fa	Dimer	0.287	0.60/0.51/0.35	−0.757	0.176	1.438	1.102
	Trimer	0.287	0.60/0.51/0.35	−0.758	0.177	1.438	1.102
	Tetramer	0.287	0.60/0.51/0.35	−0.758	0.177	1.438	1.103
	Polymer[c]	0.287	0.60/0.51/0.35	−0.761	0.177	1.438	1.169
Fb	Dimer	0.295	0.65/0.52/0.36	−0.807	0.253	1.433	1.127
	Trimer	0.296	0.65/0.52/0.36	−0.809	0.255	1.433	1.130
	Tetramer	0.296	0.65/0.52/0.36	−0.811	0.258	1.432	1.133
	Polymer[c]	0.296	0.65/0.52/0.36	−0.820	0.243	1.431	1.271
1Fc	Dimer	0.297	0.65/0.52/0.36	−0.815	0.250	1.431	1.138
	Trimer	0.298	0.66/0.52/0.36	−0.820	0.256	1.429	1.147
	Tetramer	0.300	0.66/0.52/0.36	−0.827	0.262	1.426	1.157
	Polymer[c]	0.301	0.66/0.54/0.36	−0.849	0.221	1.425	1.359
2Fc	Dimer	0.294	0.64/0.52/0.36	−0.801	0.248	1.435	1.136
	Trimer	0.296	0.65/0.52/0.36	−0.807	0.253	1.432	1.145
	Tetramer	0.297	0.65/0.52/0.36	−0.814	0.260	1.429	1.156
	Polymer[c]	0.298	0.66/0.54/0.36	−0.837	0.219	1.428	1.357
3Fc	Dimer	0.277	0.56/0.50/0.35	−0.706	0.109	1.450	1.072
	Trimer	0.277	0.56/0.50/0.35	−0.706	0.109	1.450	1.072
	Tetramer	0.277	0.56/0.50/0.35	−0.706	0.109	1.450	1.072
	Polymer[c]	0.278	0.56/0.50/0.35	−0.708	0.110	1.450	1.087

[a] See text. [b] Attained from NBO analysis. [c] One isolated structure extracted from the corresponding polymer.

3Fc, the NICS values along the polymeric axis do not change evidently because the polymeric axis is not straight. However, the NICS values in the same position, which is close to the polymeric axis, still decrease with the increase in polymeric number; for example, the NICS values of b1 in **3Fc** are 9.2, 8.4, 8.3 and 8.3 from monomer to tetramer.

The decreases in NICS (1.0 Å) values along with chain extension imply that aromatic ring currents in ring b decrease with aromatic character weakening, which suggests that the localisation potential for π-electrons in these rings is weakened, or in other words, the delocalisation potential for π-electrons along the chain is enhanced, and the outcomes lead to the enhancing of the conjugation degree for the systems, which is good for π-electrons flowing along the polymeric axis. In addition, the above analyses illustrate that the electrons in the central section do not localise on the central section but on the whole molecule.

The above analyses indicate that aromaticity is closely related to the localisation of π-electrons: the ring aromaticity is strengthened if π-electrons are localised in a ring, while ring aromaticity is weakened, but the ring current of the molecule is strengthened, if π-electrons are distributed on the whole molecule. The results also indicate that π-electrons are mainly delocalised along the polymeric axis, and π-electrons are delocalised easily with the increase in polymeric number.

Therefore, it is apparent that studying the changes in NICS values is a useful method to analyse aromatic and conjugational properties.

3.2 Periodic system

In this article, the electronic and structural properties were obtained by employing a PBC calculation. The computed one-dimensional band structures around the Fermi level are illustrated in Figure 2, and the energy gap was obtained from the minimum difference between the HOMO and LUMO energy levels at a constant k. The orbital energy can be assumed to verify the trend reliably, because the theoretical calculation in this energy level is systematic [26,27]. In the energy gap graph (Figure 2), 10 orbitals including HUMO and LUMO are displayed, and the fifth and sixth orbitals are HUMO and LUMO, respectively. The partial DOS (PDOS) spectra are shown in Figure 3. The HOMO and LUMO energies and the energy gaps of oligomers are listed in Table 3. Furthermore, the ionisation potential (IP), electronic affinity (EA) of monomers and oligomers, the bandwidths (BWs) and electron effective masses (m^*) of polymers are shown in Table 4. BW and m^* values are good parameters for predicting the hole and electron-transporting ability [28–30]. The effective mass of carriers at the band edge representing mobility was obtained as the square of $\hbar$ multiplied by the reciprocal of the curvature from $E(k)$ with k, and the formulation is

Table 2. Negative NICS for the studied compounds at 1.0 Å above (in parentheses) and at RCPs.

	Ring	Monomer	Dimer	Trimer	Tetramer
1Fa	a1	8.4 (6.5)	8.1 (6.3)	8.1 (6.3)	8.2 (6.4)
	b1	15.7 (10.9)	13.8 (9.3)	13.5 (9.1)	13.4 (9.1)
	a2			8.2 (6.4)	8.1 (6.3)
	b2			12.3 (8.1)	12.1 (7.9)
	a3			8.1 (6.4)	
	b3			13.9 (9.4)	
2Fa	a1	15.7 (10.9)	15.5 (10.6)	15.5 (10.6)	15.6 (10.7)
	b1	8.4 (6.5)	7.9 (5.9)	7.8 (5.9)	7.8 (5.9)
	a2		8.2 (6.4)	7.7 (5.8)	7.7 (5.8)
	b2		14.2 (9.7)	14.0 (9.5)	14.0 (9.5)
	a3			8.1 (6.4)	7.7 (5.8)
	b3			14.1 (9.7)	14.0 (9.5)
	a4				8.1 (6.4)
	b4				14.1 (9.7)
Fb	a1	11.7 (8.8)	11.4 (8.5)	11.3 (8.5)	11.3 (8.5)
	b1	11.7 (8.8)	10.3 (7.6)	10.3 (7.6)	10.3 (7.6)
	a2			10.1 (7.4)	10.1 (7.4)
	b2			10.1 (7.4)	10.0 (7.4)
1Fc	a1	12.3 (9.2)	11.9 (8.9)	11.9 (8.9)	11.8 (8.8)
	b1	12.3 (9.2)	10.9 (8.0)	10.8 (8.0)	10.8 (8.0)
	a2			10.6 (7.7)	10.6 (7.6)
	b2			10.6 (7.7)	10.5 (7.7)
2Fc	a1	12.3 (9.2)	11.9 (8.9)	11.8 (8.8)	11.8 (8.8)
	b1	12.3 (9.2)	11.2 (8.2)	11.1 (8.1)	11.1 (8.1)
	a2			10.8 (7.8)	10.8 (7.8)
	b2			10.8 (7.8)	10.8 (7.8)
3Fc	a1	12.3 (9.2)	12.2 (9.1)	12.2 (9.1)	12.2 (9.1)
	b1	12.3 (9.2)	11.2 (8.4)	11.1 (8.3)	11.1 (8.3)
	a2			11.1 (8.2)	11.1 (8.2)
	b2			11.1 (8.2)	11.1 (8.2)

defined as

$$\frac{1}{m^*} = \frac{1}{\hbar^2}\left(\frac{\partial^2 E(k)}{\partial k^2}\right). \quad (1)$$

The kinetic model of mobility (μ) is given by the following formula:

$$\mu = \frac{eT}{m^*}. \quad (2)$$

According to the band theory, the wider the BW, the smaller the effective mass, and the larger the kinetic model of mobility [31].

3.2.1 *PFa*

PFa contains two kinds of polymeric form, **1PFa** and **2PFa**, and both **1PFa** and **2PFa** are coplanar molecules.

In the case of **1PFa**, the polymeric axis is straight, which is in favour of the flow of electrons. From Table 3, we can easily see that the energy gaps decrease gradually with the increase in polymeric number (from monomer to tetramer: 5.20, 3.50, 2.92 and 2.45 eV, respectively). In contrast to oligomers, the HOB energy of polymer **1PFa** is larger than the HOMO energies of oligomers, while the LUB energy of polymer **1PFa** is smaller than that of the corresponding oligomers; therefore, the energy gap of polymer **1PFa** is smaller (1.21 eV) than oligomers, which indicates that energy gaps decrease with the increase in polymeric number. From Table 4, we can find that the IP values of **1Fa** are smaller but the EA values are larger with the increase in polymeric number, and the change in trends is shown in Figures 4 and 5, which suggests that the ability of the compound gaining electrons increases with the increase in polymeric number.

As shown in Figure 2, there is an item gap between the bottom of LUB and the top of HOB, which indicates that there are no orbital overlaps between the top of HOB and the bottom of LUB, and it is an indirect energy gap. Meanwhile, the band curves near -3 eV (the top of the occupied band and the bottom of the vacant band) bend greatly with the change in k value; correspondingly, the peak in the DOS graph (Figure 3) changes moderately, which illustrates that the localisation of the orbital is stronger. In contrast, except for the top of HUB and the

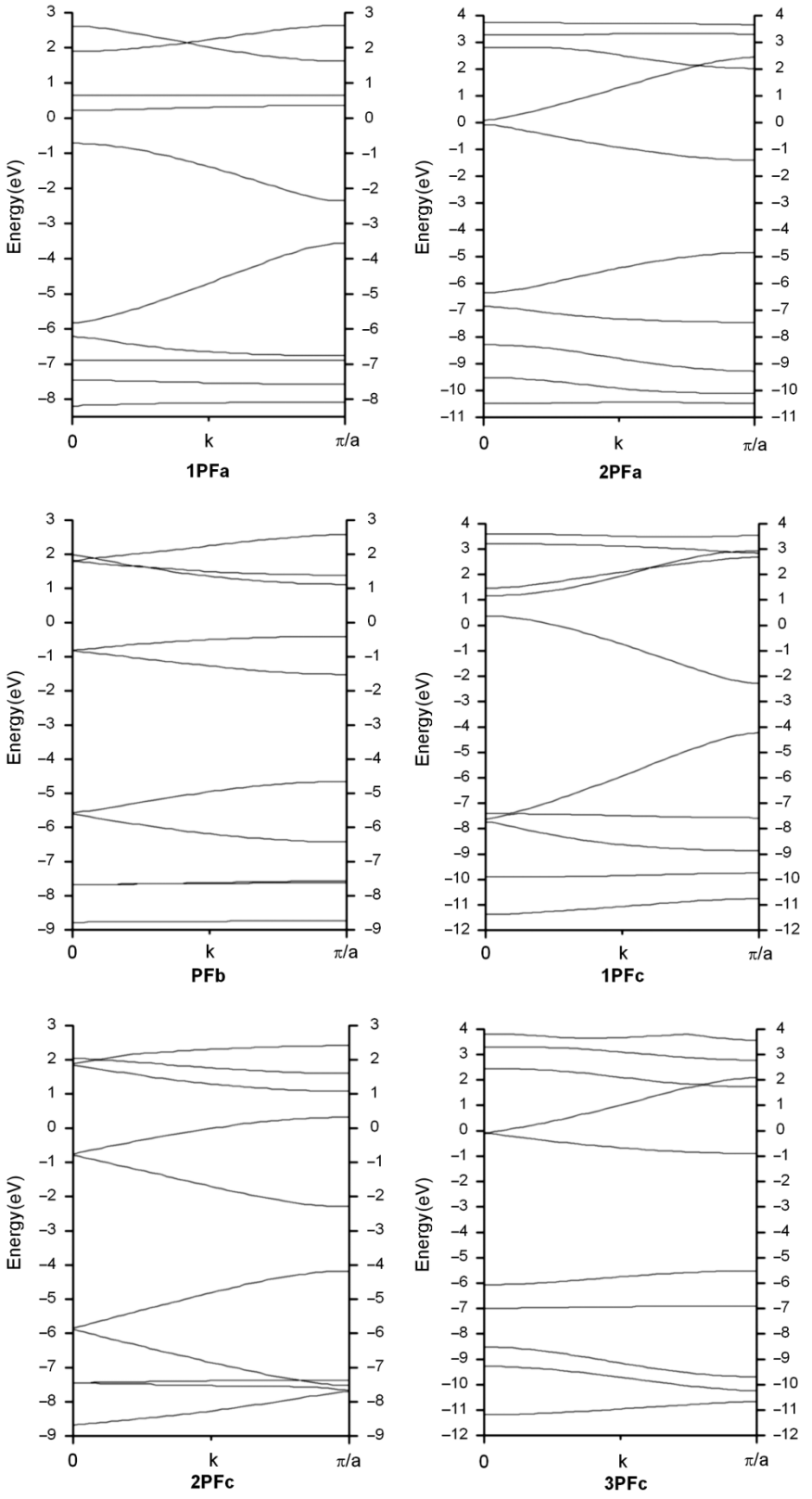

Figure 2. Band structures of **PF1**, **PF2**, **PF3** and **PF4**.

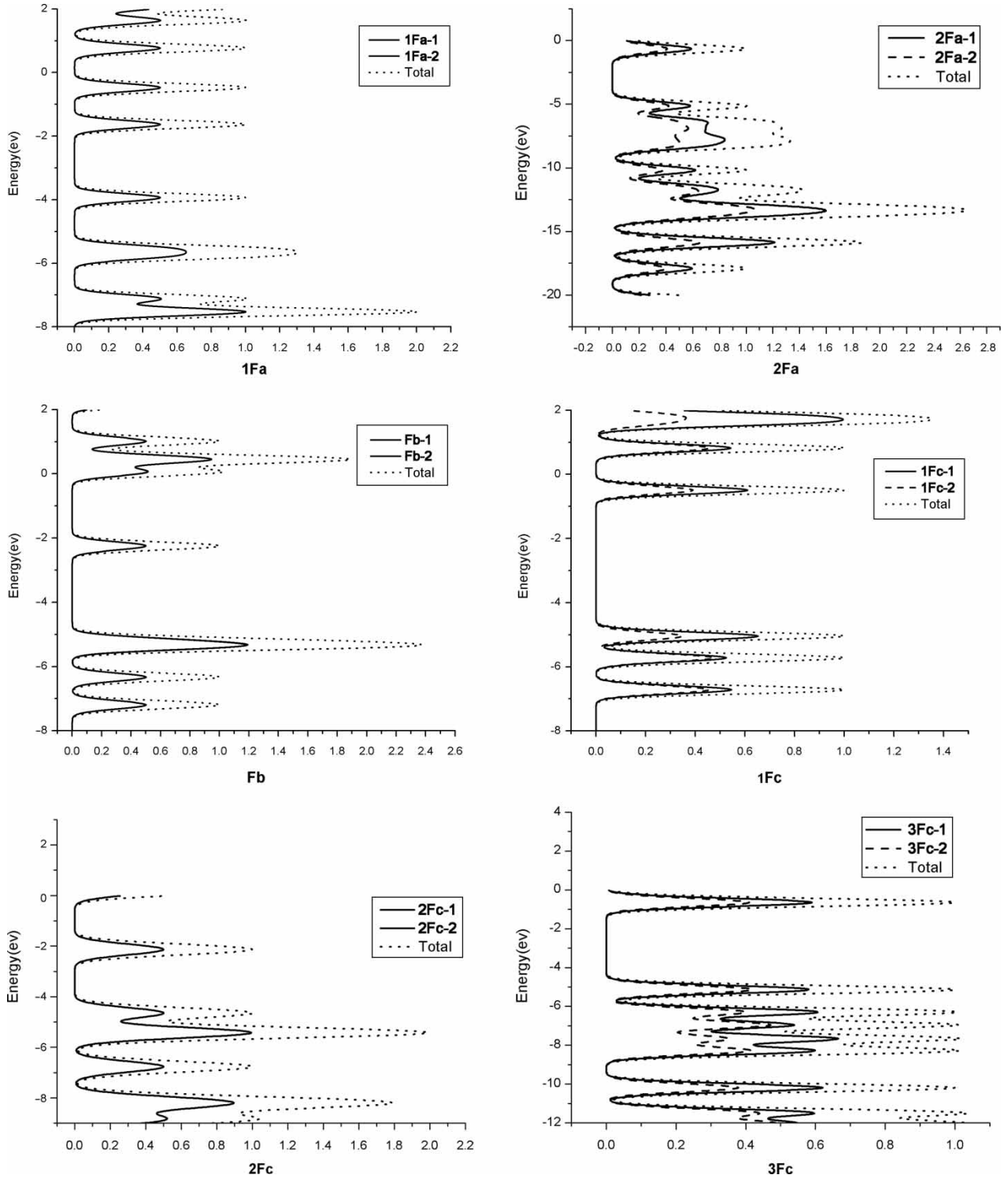

Figure 3. DOS and PDOS of one isolated structure extracted from polymers.

bottom of LUB, the other bands are even, and the DOS spectra show that the corresponding peaks are sharp, which suggests that the bonding function is relatively weak. Since the structures of the two radical groups, **1Fa-1** and **1Fa-2**, are completely identical, their PDOSs are overlapped completely. As shown in Table 4, the larger BW (conduction band: 1.361 eV; valence band: 1.932 eV, respectively), the smaller effective mass (m^*; conduction

Table 3. Energy (eV) of HOMO and LUMO, energy gaps for oligomers and band gaps for polymers.

		Monomer	Dimer	Trimer	Tetramer	Polymer
1Fa	H	−5.56	−4.75	−4.38	−4.19	−3.56
	L	−0.36	−1.25	−1.46	−1.74	−2.35
	E_g	5.20	3.50	2.92	2.45	1.21
2Fa	H	−5.56	−5.04	−4.91	−4.86	−4.84
	L	−0.36	−0.93	−1.13	−1.23	−1.39
	E_g	5.20	4.11	3.78	3.63	3.45
Fb	H	−5.73	−5.03	−4.84	−4.76	−4.65
	L	0.41	−0.77	−1.06	−1.21	−1.51
	E_g	6.14	4.26	3.78	3.55	3.14
1Fc	H	−5.57	−4.89	−4.63	−4.49	−4.22
	L	−0.09	−1.16	−1.56	−1.78	−2.29
	E_g	5.48	3.73	3.07	2.71	1.93
2Fc	H	−5.57	−4.88	−4.61	−4.47	−4.19
	L	−0.09	−1.17	−1.57	−1.78	−2.30
	E_g	5.48	3.71	3.04	2.69	1.89
3Fc	H	−5.57	−5.45	−5.44	−5.45	−5.51
	L	−0.09	−0.51	−0.67	−0.75	−0.91
	E_g	5.48	4.94	4.77	4.70	4.60

Note: For polymer, H means HOB and L means LUB.

BW: 0.698 eV; valence BW: 0.646 eV, respectively) along with larger kinetic model of mobility (μ) lead to small energy gap. The energy gap of **1PFa** is 1.21 eV.

In the case of **2PFa**, the polymeric axis is flexural, and the electron does not flow easily as for **1PFa**, therefore the energy gap of **2PFa** is larger than that of **1PFa**. However, the change in trend of the energy gaps is the same as that for **1PFa** (monomer > dimer > trimer > tetramer). The HOMO energy increases with the increase in polymeric number, while the LUMO energy decreases, which results

Table 4. IP (Hartree), EA (Hartree), BW (eV) and effective mass (m^*).

	Polymeric number	IP	EA	Conduction band of the polymer		Valence band of the polymer	
				BW	m^*	BW	$-m^*$
1Fa	Monomer	0.281	0.045	1.361	0.698	1.932	0.646
	Dimer	0.232	0.002				
	Trimer	0.209	−0.014				
	Tetramer	0.196	−0.03				
2Fa	Monomer	0.281	0.045	1.306	1.919	1.497	1.352
	Dimer	0.243	0.012				
	Trimer	0.230	−0.002				
	Tetramer	0.222	−0.011				
Fb	Monomer	0.285	0.063	0.571	3.235	0.844	2.841
	Dimer	0.241	0.017				
	Trimer	0.242	−0.002				
	Tetramer	0.216	−0.012				
1Fc	Monomer	0.280	0.051	2.340	0.256	2.721	0.256
	Dimer	0.236	0.002				
	Trimer	0.216	−0.02				
	Tetramer	0.203	−0.034				
2Fc	Monomer	0.280	0.051	1.497	1.384	1.660	1.384
	Dimer	0.235	0.001				
	Trimer	0.215	−0.021				
	Tetramer	0.204	−0.034				
3Fc	Monomer	0.280	0.051	0.789	3.662	0.544	3.639
	Dimer	0.257	0.025				
	Trimer	0.248	0.012				
	Tetramer	0.241	0.004				

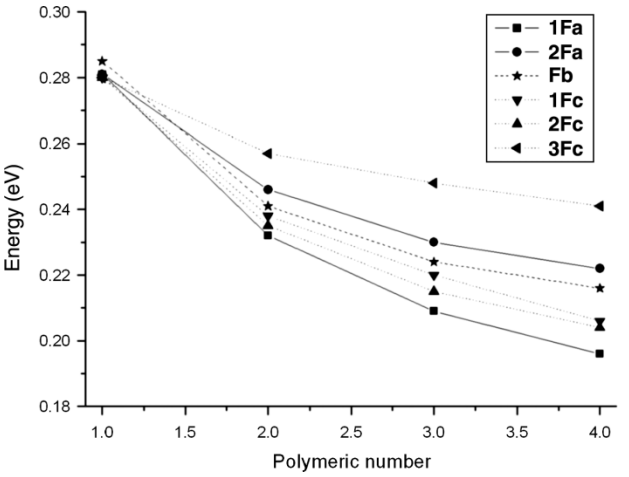

Figure 4. IP of **1Fa**, **2Fa**, **Fb**, **1Fc**, **2Fc** and **3Fc** (the points from 1 to 4 denote monomer, dimer, trimer and tetramer, respectively).

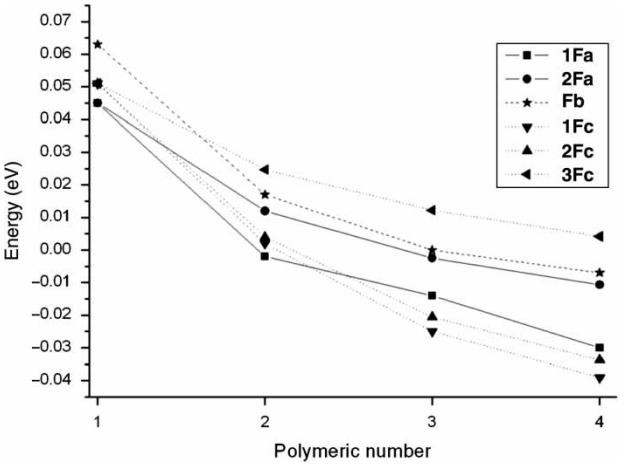

Figure 5. EA of **1Fa**, **2Fa**, **Fb**, **1Fc**, **2Fc** and **3Fc** (the points from 1 to 4 denote monomer, dimer, trimer and tetramer, respectively).

in the above change in trend of energy gaps. Furthermore, BW is smaller and m^* is larger than those for **1PFa** (conduction BW: 1.306 eV, m^*: 1.919 m_e; valence BW: 1.479 eV, m^*: 1.352 m_e, respectively); according to formula (2), the kinetic model of mobility (μ) is smaller than that for **1PFa**, which results in larger energy gap than that for **1PFa** (**2PFa**: 3.45 eV). From Figure 2, we also find that the conduction and valence bands are moderate and the energy gaps are large.

3.2.2 PFb

In contrast to **1PFa** and **2PFa**, the polymeric form of **PFb** is different though the polymeric axis is straight. In a unit, the two oxygen atoms are located in the same side of the furan rings. The data in Table 3 indicate that the energy gaps decrease with the increase in polymeric number (from monomer to tetramer: 6.14, 4.26, 3.78 and 3.55 eV, respectively), which results from the increase in HOMO energy and the decrease in LUMO energy (HOMO: −5.73, −5.03, −4.84, −4.76 and −4.65 eV, LUMO: 0.41, −0.77, −1.06, −1.21 and −1.51 eV). Meanwhile, the data in Table 4 suggest that the narrower band corresponds to larger m^* but smaller μ. The profiles in Figures 2 and 3 illustrate the same results. The energy gap curves of the selected front-line orbitals are moderate, and the corresponding peaks in the DOS graph are relatively sharp. This indicates that the localisation degree of the orbitals is small, and the interactions between the orbitals are weak, which is not advantageous for electronic locations, at the same time it also affects the conductive properties of the polymer. The band gap of **PFb** is 3.14 eV.

3.2.3 PFc

On the basis of **Fc**, there are three kinds of polymeric forms leading to **1PFc**, **2PFc** and **3PFc**; **1PFc** and **2PFc** have the same polymeric form.

For **1PFc**, the oxygen atoms lie on the two sides of the furan rings equally, and the polymeric axis is straight. Inspection of Table 3 shows that the energy gaps decrease with the increase in polymeric number (from monomer to tetramer: 5.48, 3.73, 3.07 and 2.71 eV), and the energy gap of **1PFc** is 1.93 eV. The values of BW and m^* show that **1PFc** has a wide band gap and small m^* (conduction BW: 2.340 eV, m^*: 0.256 m_e; valence BW: 2.721 eV, m^*: 0.256 m_e). From Figure 2, we find that there are no orbital overlaps. Hence, the energy gap belongs to an indirect energy gap as well. The other band curves are even, especially the curves which are near 2 eV and after 7 eV are relatively straight. Furthermore, the corresponding sharp peaks are displayed in Figure 4. It suggests that the localisations of HOB and LUB are strong, and the interaction between the orbitals is also strong, which are good for the localisation of electrons and conductive ability.

2PFc has the same polymeric form as **1PFc** and the polymeric axis is also straight. The HOMO energy increases with the increase in polymeric number, while the LUMO energy decreases, hence the energy gaps decrease with the increase in polymeric number (from monomer to tetramer: 5.48, 3.71, 3.04 and 2.69 eV, respectively). The BW and m^* values listed in Table 4 suggest that the valence band is wider than the conduction band while both of them have the same m^* values. The above values indicate that the relationship between band gap and m^* is not absolutely consistent, because the m^* values are also affected by many factors. From Figures 2 and 3, we can see that the band gap centres on −2 to −4 eV, and the energy gap of **2PFc** is 1.89 eV.

The last polymer of **Fc** is **3PFc**, and the polymeric axis is flexural, which is not good for the electron flow, therefore **3PFc** has larger band gap in contrast to the other five polymers. As shown in Table 3, the HOMO energy is smaller and the LUMO energy is larger compared with the other oligomers. However, the change in trend is the same as for the above polymers. The band structure of Figure 2 illustrates that the energy gap centres on -1 to -5 eV, and the curves on the corresponding positions in Figure 3 are moderate, which illustrates that the localisation of the orbital is stronger. Furthermore, the BW and m^* values of the polymers shown in Table 4 suggest that **3PFc** has the most narrow band, the largest m^* and the smallest μ (BW: 0.789 eV and m^*: 3.662 m_e for the conduction band; BW: 0.544 eV and m^*: 3.639 m_e for the valence band). Therefore, **3PFc** has the largest band gap, which is 4.60 eV.

The energy gap, BW, m^*, kinetic model of mobility and the DOS analyses for oligomers and polymers give us a more useful way to understand the electronic properties of the structure, thereby we can further study the conductive properties.

4. Conclusions

In this article, electronic and structural properties of the three bicyclical classical furans, **Fa**, **Fb** and **Fc**, are studied in detail. The DFT theoretical method is employed to calculate monomers, oligomers and polymers. By analysing the NICS changes at RCPs, the BCP properties and the WBIs in the central bands, we find that the aromaticity is degressive and the conjugational degree increases with the increase in polymeric number; meanwhile, the conjugational degree in the central part is stronger than that in the outer part. Furthermore, the BW, m^* values and energy gaps suggest that the polymers of **1PFa**, **1PFc** and **2PFc** have larger BW values and smaller m^* values than **2PFa**, **PFb** and **3PFc**, which is basically in accordance with the energy gap (**1PFa**: 1.21 eV, **2PFa**: 3.45 eV, **PFb**: 3.14 eV, **1PFc**: 1.93 eV, **2PFc**: 1.89 eV and **3PFc**: 4.60 eV, respectively) Therefore, the above analyses illustrate that **1PFa**, **1PFc** and **2PFc** are good candidates for conductive materials.

Acknowledgements

This work was supported by the Boshi Dian Foundation of Ministry of Education (Grant No. 200806350013), the Natural Science Foundation Project of CQ CSTC (Grant No. CSTC, 2009BB4104) and the Applied Basic Foundation of Chongqing Municipal Commission of Education (Grant No. KJ071302). We are grateful to the anonymous referees for their suggestions.

References

[1] H. Shirakawa, E.J. Louis, A.G. MacDiarmid, C.K. Chiang, and A.J. Heeger, *Synthesis of electrically conducting organic polymers: Halogen derivatives of polyacetylene, $(CH)_x$*, J. Chem. Soc. Chem. Commun. 16 (1977), pp. 578–580.

[2] C.K. Chiang, C.R. Fincher, Jr, Y.W. Park, A.J. Heeger, H. Shirakawa, E.J. Louis, S.C. Gau, and A.G. MacDiarmid, *Electrical conductivity in doped polyacetylene*, Phys. Rev. Lett. 39 (1977), pp. 1098–1101.

[3] P. Bäuerle, *Intrinsically conducting polymers – Quo vadis?* Adv. Mater. 5 (1993), pp. 879–886.

[4] J. Roncali, *Synthetic principles for bandgap control in linear p-conjugated systems*, Chem. Rev. 97 (1997), pp. 173–205.

[5] S.J. Higgins, *Conjugated polymers incorporating pendant functional groups – Synthesis and characterization*, Chem. Soc. Rev. 26 (1997), pp. 247–258.

[6] J. Roncali, *Electrogenerated functional conjugated polymers as advanced electrode materials*, J. Mater. Chem. 9 (1999), pp. 1875–1893.

[7] W. Shen, M. Li, R. He, J. Zhang, and W. Lei, *The electronic and structural properties of nonclassical bicyclic thiophene: Monomer, oligomer and polymer*, Polymer 48 (2007), pp. 3912–3918.

[8] J.C. Jung, J.-C. Kim, H.-I. Moon, and S. Park, *Stereoselective total synthesis of furofuran lignans through dianion aldol condensation*, Tetrahedron Lett. 47 (2006), pp. 6433–6437.

[9] J.I. Aihara, *Aromaticity and stability of furofurans and thienothiophenes*, J. Phys. Org. Chem. 18 (2005), pp. 235–239.

[10] W. Eberbach and J. Roser, *Thermally initiated reactions of (Z)-epoxyhexenynes. A facile preparation of 3,4-annulated furans*, Tetrahedron 42 (1986), pp. 2221–2234.

[11] J. Vader, H. Sengers, and A. de Groot, *The stereoselective syntheses of substituted furo[2,3b]furan. (Part II)*, Tetrahedron 45 (1989), pp. 2131–2142.

[12] P. Tuchinda, B. Munyoo, M. Pohmakotr, P. Thinapong, S. Sophasan, T. Santisuk, and V. Reutrakul, *Cytotoxic styryl-lactones from the leaves and twigs of* Polyalthia crassa, J. Nat. Prod. 69 (2006), pp. 1728–1733.

[13] P.v.R. Schleyer, C. Maerker, A. Dransfeld, H. Jiao, and N.J.R. van Eikema Hommes, *Nucleus-independent chemical shifts: A simple and efficient aromaticity probe*, J. Am. Chem. Soc. 118 (1996), pp. 6317–6318.

[14] R.G. Parr and W. Yang, *Density-functional Theory of Atoms and Molecules*, University Press, Oxford, New York, 1989.

[15] A.D. Becke, *Density-functional thermochemistry. III. The role of exact exchange*, J. Chem. Phys. 98 (1993), pp. 5648–5652.

[16] C. Lee, W. Yang, and R.G. Parr, *Development of the Colle–Salvetti correlation-energy formula into a functional of the electron density*, Phys. Rev. B 37 (1988), pp. 785–789.

[17] K.N. Kudin and G.E. Scuseria, *Linear-scaling density-functional theory with Gaussian orbitals and periodic boundary conditions: Efficient evaluation of energy and forces via the fast multipole method*, Phys. Rev. B 61 (2000), pp. 16440–16453.

[18] M.J. Frisch, G.W. Trucks, H.B. Schlegel, G.E. Scuseria, M.A. Robb, J.R. Cheeseman, J.A. Montgomery, Jr, T. Vreven, K.N. Kudin, J.C. Burant, J.M. Millam, S.S. Iyengar, J. Tomasi, V. Barone, B. Mennucci, M. Cossi, G. Scalmani, N. Rega, G.A. Petersson, H. Nakatsuji, M. Hada, M. Ehara, K. Toyota, R. Fukuda, J. Hasegawa, M. Ishida, T. Nakajima, Y. Honda, O. Kitao, H. Nakai, M. Klene, X. Li, J.E. Knox, H.P. Hratchian, J.B. Cross, C. Adamo, J. Jaramillo, R. Gomperts, R.E. Stratmann, O. Yazyev, A.J. Austin, R. Cammi, C. Pomelli, J.W. Ochterski, P.Y. Ayala, K. Morokuma, G.A. Voth, P. Salvador, J.J. Dannenberg, V.G. Zakrzewski, A.D. Daniels, O. Farkas, A.D. Rabuck, K. Raghavachari, J.V. Ortiz, *Gaussian 03, revision A.1*, Gaussian, Inc., Pittsburgh, PA, 2003.

[19] R.F.W. Bader, *Atoms in Molecules, A Quantum Theory*, 22, International Series of Monographs in Chemistry, Vol. 22, Oxford University Press, Oxford, UK, 1990.

[20] N.M. O'Boyle and J.G. Vos, *GaussSum 1.0*, Dublin City University, 2005. Available at http://gausssum.sourceforge.net.

[21] G. Herlem and B. Lakard, Ab initio *study of the electronic and structural properties of the crystalline polyethyleneimine polymer*, J. Chem. Phys. 120 (2004), pp. 9376–9382.

[22] A.E. Reed, R.B. Weinstock, and F. Weinhold, *Natural population analysis*, J. Chem. Phys. 83 (1985), pp. 735–746.

[23] W.X. Zheng, N.-B. Wong, W.Z. Wang, G. Zhou, and A. Tian, *Theoretical study of 1,3,4,6,7,9,9b-heptaazaphenalene and its ten derivatives*, J. Chem. Phys. 108 (2004), pp. 97–106.

[24] P.v.R. Schleyer, M. Manoharan, Z.-X. Wang, B. Kiran, H. Jiao, R. Puchta, and N.J.R. van Eikema Hommes, *An evaluation of the aromaticity of inorganic rings: Refined evidence from magnetic properties*, J. Am. Chem. Soc. 119 (1997), pp. 12669–12670.
[25] P.v.R. Schleyer, M. Manoharan, Z.X. Wang, B. Kiran, H. Jiao, R. Puchta, and N.J. van Eikema Hommes, *Dissected nucleus-independent chemical shift analysis of p-aromaticity and anti-aromaticity*, Org. Lett. 3 (2001), pp. 2465–2468.
[26] U. Salzner, *Theoretical analysis of poly(difluoroacetylene)*, J. Phys. Chem. B 107 (2003), pp. 1129–1134.
[27] U. Salzner, P.G. Pickup, and R.A. Poirier, *Accurate method for obtaining band gaps in conducting polymers using a DFT/hybrid approach*, J. Phys. Chem. A 102 (1998), pp. 2572–2578.
[28] R.C. Haddon, T. Siegrist, R.M. Fleming, P.M. Bridenbaugh, and R.A. Laudise, *Band structures of organic thin-film transistor materials*, J. Mater. Chem. 5 (1995), pp. 1719–1724.
[29] J. Cornil, J.Ph. Calbert, and J.L. Bredas, *Electronic structure of the pentacene single crystal: Relation to transport properties*, J. Am. Chem. Soc. 123 (2001), pp. 1250–1251.
[30] Y.C. Cheng, R.J. Silbey, D.A. da Silva Filho, J.P Calbert, J. Cornil, and J.L. Brédas, *Three-dimensional band structure and bandlike mobility in oligoacene single crystals: A theoretical investigation*, J. Chem. Phys. 118 (2003), pp. 3764–3774.
[31] J.G. Zhu, W.C. Zheng, J.G. Zheng, X.S. Sun, H.T. Wang, *Solid Physics*, Science Press, 2005.